Development of a Flexible SU-8/PDMS-Based Antenna

Chih-Peng Lin, Chieh-Hsiang Chang, Y. T. Cheng, *Senior Member, IEEE*, and Christina F. Jou

***Abstract*—In this letter, a flexible SU-8/PDMS-based antenna has been demonstrated, not only targeting the wearable computing, but also fitting well in the RF system-on-package (RF SOP) applications. The characteristics of the proposed antenna fabricated on a flexible polymer substrate (SU-8/PDMS) with different bending angles have been successfully measured and characterized for the first time. The measured results have shown fairly good agreement with the simulation results. The measured bandwidth and maximum gain are 3% from 6.2 to 6.4 GHz and 2.17 dBi, respectively, when the antenna is flat. Moreover, related antenna fabrication process provides a practical approach to realize the flexible antenna for the portable wireless electronics applications.**

***Index Terms*—Flexible electronics, microstrip antenna, polydimethylsiloxane (PDMS), planar antenna, SU-8.**

I. Introduction

FLEXIBLE electronics have drawn significant attention in the past decades. More and more flexible electronics have been developed, such as flexible displays, smart tags, and wearable products. Steady progress in developing flexible microelectronics along with other new technologies can enable functionality integration. To realize these goals, flexible ICs have become a must technology for portable wireless applications [1], [2]. One of the technical challenges to the technology is how to well integrate passive components with active components on the same flexible substrate that can simultaneously reduce package size and weight and offer better microwave performance with good energy efficiency.

Numerous approaches have been proposed in the prior decade by utilizing different materials as flexible substrates [3]–[5]. In these approaches, a variety of polymer materials (e.g., LCP, PEI, and PET) have been chosen as the substrate for the flexible electronic applications owing to the attractive RF characteristics of low relative dielectric constants, low dissipation factors, and capability of being laminated [5]. Meanwhile, polymers such as polydimethylsiloxane (PDMS) and SU-8 have been widely adopted for microwave microsystem fabrication in recent years [6]–[9]. PDMS as microwave frequency electronics' substrate has several promising features, such as good chemical stability and low dielectric constant. PDMS can also be attached to other substrate materials via surface treatment of oxygen plasma. The SU-8 photoresist, first introduced by IBM for printed circuit board applications, has been widely used in micromachining, packaging, and other microelectronics areas, for microwave and RF applications. The investigations about the high-frequency properties of SU-8 such as low dielectric constant and loss tangent have also revealed its feasibility for wireless applications [8], [9].

Previously, we demonstrated a heterogeneous chip integration technology using an SU-8/PDMS substrate where a compact flexible microsystem can be realized without having any material and process limits. Discrete components are designed and fabricated on separate chips, and then fully integrated onto a flexible substrate to form a microsystem [10], [11]. Since it is a wafer-level chip-scale fabrication scheme for flexible wireless microsystem applications using the sacrificial release process and low-temperature bumpless Au-Au thermocompressive (TC) bonding technology, low-cost, reliable, flexible wireless microsystems with a small form factor can indeed be fully realized. In addition, not only CMOS chips, but also the other heterogeneous chips, like MEMS and III-V chips, can be fully integrated with a flexible organic substrate using the proposed scheme to form a high-performance wireless microsystem.

A few flexible antenna technologies and research have been conducted. For instance, Locher *et al.* [12] designed and characterized purely textile patch antenna using conductive fabric. Cheng *et al.* [13], [14] demonstrated a foldable and stretchable liquid metal planar inverted cone and unbalanced loop antenna. Apaydin *et al.* [15] introduced a printing technique to fabricate a microstrip patch antenna printed on PDMS-ceramic composites. Nevertheless, none of the studies have shown the capability of batch processing and direct heterogeneous chip integration to form a miniature wireless microsystem with the aforementioned features including smaller form factor, lower manufacture cost, and better RF characteristics. In order to further demonstrate the technique we have proposed for flexible RF electronics fabrication, this letter presents the development of microstrip patch antenna fabricated on the flexible polymer SU-8/PDMS substrate. In addition, the related bending effect will also be investigated since the occurrence of antenna bending would be very common in most personal portable device applications, and it would result in a critical effect on the antenna in terms of the radiation characteristic change, especially when the antenna size becomes smaller.

II. Antenna Design

Targeting wearable application, a planar patch antenna is considered more practical than other types of antennas. The design of the patch antenna is fairly simple and can further simplify the measurement using a microstrip feed. Therefore, a microstrip

Manuscript received August 11, 2011; accepted September 16, 2011. Date of publication October 03, 2011; date of current version October 17, 2011. This work was supported in part by the Ministry of Economic Affairs of Taiwan under Grant 99-EC-17-A-03-S1-005 and the Ministry of Education in Taiwan under the ATU Program.

C.-P. Lin, C.-H. Chang, and C. F. Jou are with the Department of Communication Engineering, National Chiao Tung University, Hsinchu 30010, Taiwan (e-mail: jadanz.cm96g@g2.nctu.edu.tw; christinajou3@gmail.com).

Y.-T. Cheng is with the Electronics Engineering, Department of National Chiao Tung University, Hsinchu, Taiwan (e-mail: ytcheng@mail.nctu.edu.tw).

Color versions of one or more of the figures in this letter are available online at http://ieeexplore.ieee.org.

Digital Object Identifier 10.1109/LAWP.2011.2170398

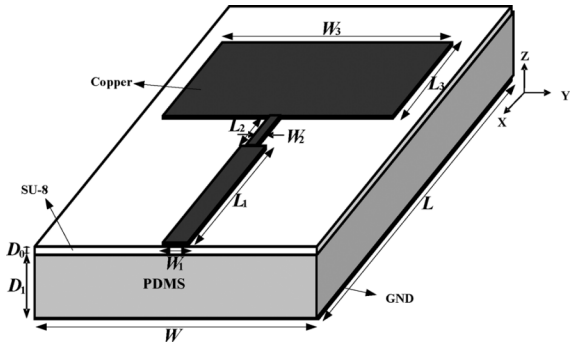

Fig. 1. Schematic view of the flexible SU-8/PDMS microstrip patch antenna with optimized dimensions: $W = 20$ mm, $L = 46.4$ mm, $W_1 = 1.35$ mm, $W_2 = 0.8$ mm, $W_3 = 17.36$ mm, $L_1 = 20$ mm, $L_2 = 6$ mm, $L_3 = 14.4$ mm, $D_0 = 50$ μm, and $D_1 = 500$ μm.

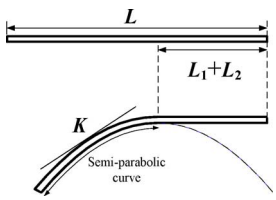

Fig. 2. Assumption of the bending configuration.

patch antenna has been chosen in our design. Rough design estimation can be made using (1) and (2), given in [16] to determine the resonant frequency and the input impedance, respectively. $\varepsilon_{\rm r}$ is the dielectric constant of the substrate. The geometrical view of the proposed antenna is shown in Fig. 1

$$L_3 \approx 0.49\lambda_d = 0.49\frac{\lambda}{\sqrt{\varepsilon_{\rm r}}} \tag{1}$$

$$Z_{\rm A} = 90\frac{{\varepsilon_{\rm r}}^2}{\varepsilon_{\rm r} - 1}\left(\frac{L_3}{W_3}\right)\ \Omega. \tag{2}$$

The size of the feed line ($W_1 \times L_1$) is designed to meet 50 Ω. The extra strip ($W_2 \times L_2$) is added to improve the matching between the patch and the feed line. The design of the proposed antenna is first estimated by the equations as aforementioned, and then the full-wave electromagnetic Ansoft High-Frequency Structure Simulator (HFSS) is utilized to optimize the design.

The flexible substrate of the proposed antenna is composed of a 50-μm-thick photoresist SU-8 ($\varepsilon_{\rm r} = 2.9$, $\tan\delta = 0.04$ up to 15 GHz) [8] in the upper layer and a 500-μm-thick PDMS ($\varepsilon_{\rm r} = 2.65$, $\tan\delta = 0.02$) below to offer a better mechanical support for the SU-8 layer. The considered PDMS is the Dow Corning's Sylgard 184 specified with $\varepsilon_{\rm r} = 2.65$ and $\tan\delta = 0.001$ up to 100 kHz only. Nicolas *et al.* [6] have calculated the parameters over 72–82 GHz ($\varepsilon_{\rm r} = 2.672$, $\tan\delta = 0.0375$), therefore the assumption of $\varepsilon_{\rm r} = 2.65$ and $\tan\delta = 0.02$ for PDMS is used for the simulation. The radiating patch and the feed line are fabricated on top of the SU-8 layer. The ground plane is fabricated underneath the PDMS layer. The curvature of the proposed antenna with corresponding geometrical parameters is shown in Fig. 2. The curvature K is calculated at the midpoint of a semi-parabolic curve, which resembles our experimental samples in the bended conditions. Fig. 3 shows the simulated reflection coefficients of the proposed antenna with different curvature K. The resonant frequency decreases as the curvature increases. The antenna fails as K approaches 71.78. More detail of the

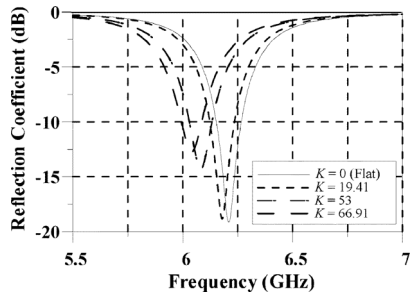

Fig. 3. Simulated reflection coefficient of the proposed antenna with different curvature K.

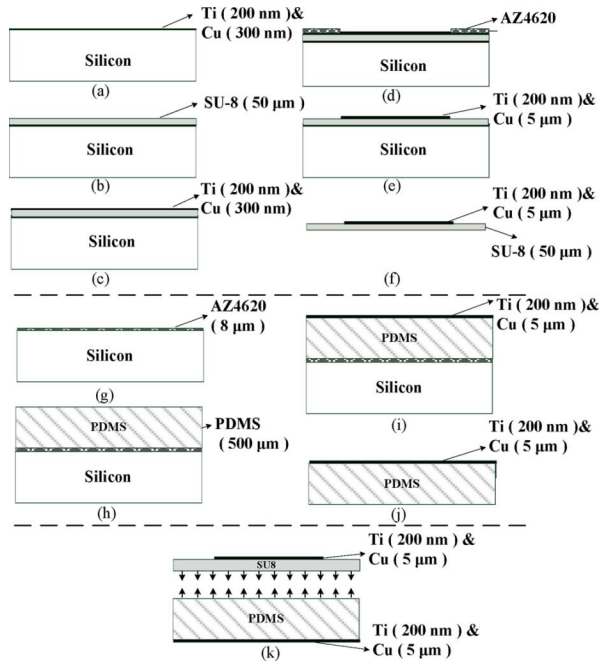

Fig. 4. Fabrication process flow of the proposed antenna.

bending effect on the electrical performance of the proposed antennas will be discussed in Section IV. The overall size ($W \times L$) of the proposed antenna is 20×46.4 mm^2.

III. Antenna Fabrication

Fig. 4 illustrates the whole fabrication process flow of the proposed antenna, which can be divided into three parts. The first part is to fabricate radiating element on the SU-8 substrate: The titanium and copper layers are sputtered on the silicon wafer as the sacrificial layer [see Fig. 4(a)]. SU-8 is coated on the sacrificial layer and defined by photolithography as the top layer of the antenna substrate [see Fig. 4(b)]. A thin 200-nm titanium-adhesion-layer and a 300-nm copper-seed-layer are sputtered on the patterned SU-8 layer [see Fig. 4(c)]. The deposited metal is patterned using photoresist AZ 4620 as a mask, and then electroplated with a 5-μm-thick Cu layer [see Fig. 4(d)]. The photoresist is removed by acetone, and then the removal of Cu in the unwanted region will be done by Cu etchant (100:5:5 H_2O:CH_3COOH:H_2O_2) to form the patch [see Fig. 4(e)]. Finally, another photoresist AZ4620 is coated on the patch and then baked for 30 min at 90°C to protect the Cu pattern on the SU-8 substrate from the following sacrificial release dipped in Cu etchant for approximately 2 h to chemically etch away

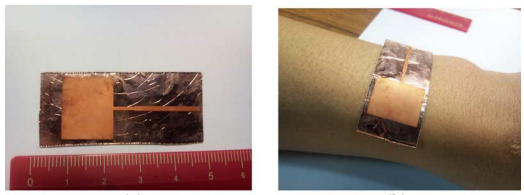

(a) (b)

Fig. 5. Photographs of (a) the proposed antenna and (b) the proposed antenna circled around the wrist.

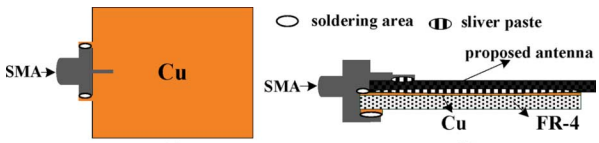

(a) (b)

Fig. 6. Schematic views. (a) Top view of the FR-4 holder. (b) Cross-sectional view of the proposed antenna attached with the FR-4 holder.

the sacrificial Ti/Cu layer underneath the SU-8 substrate [see Fig. 4(f)]. The second part is to fabricate the ground plane on the PDMS substrate: A photoresist AZ4620 is coated on a silicon substrate as a sacrificial layer [see Fig. 4(g)]. A 500-μm-thick PDMS is then spin-coated on the substrate with 100 rpm for 60 s [see Fig. 4(h)]. Ti/Cu is sputtered on the PDMS as the seed layer for Cu electroplating. About 5-μm-thick electroplated Cu is to serve as the ground plane of the patch antenna [see Fig. 4(i)]. The PDMS substrate is released from the silicon wafer using acetone [see Fig. 4(j)].

In the last part, the PDMS surface is cleaned by isopropyl alcohol and deionized water rinse and then directly attached to the SU-8 substrate as a supporting substrate to complete the process [see Fig. 4(k)]. Fig. 5(a) and (b) shows photographs of the as-fabricated flexible SU-8/PDMS microstrip patch antenna and the sample fitted in a human's wrist, respectively.

IV. Measurement Setup, Results, and Discussion

A. Setup for Measurements

In general, the feed line and ground plane of the microstrip patch antenna fabricated on the printed circuit board (PCB) substrate are soldered with an SMA connector in order to conduct the measurement. However, in our case, the microstrip feed line fabricated on the SU-8 layer will be easily torn apart due to the high-temperature soldering process. In order to solve this problem, a 1.6-mm-thick FR-4 holder with copper on both sides is soldered with the SMA connector in advance, and then the proposed antenna is attached with the holder using sliver paste as shown in Fig. 6. The silver paste is utilized to replace the high-temperature soldering process. The ground leg of the SMA connector is soldered at the bottom of the FR-4 holder.

B. Results and Discussion

The S_{11} of the proposed antenna was measured through HP 8722C vector network analyzer. The proposed antenna is bent into four different curvatures for the measurement. Fig. 7 shows photographs of the proposed antenna with different bending level installed on the measurement equipment. Fig. 8 shows the measured S_{11} of the proposed antenna with approximate K from 0 to 66.91. In comparison to the antenna without being bent, the resonant frequencies go down as the

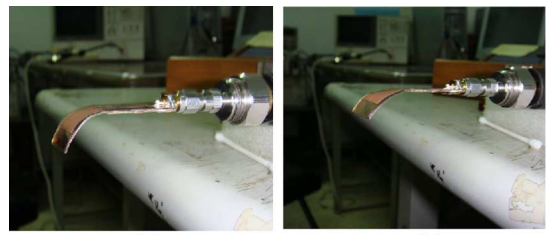

(a) (b)

Fig. 7. Photographs of the proposed antenna with different bending level. K approximately equals (a) 66.91 and (b) 53.

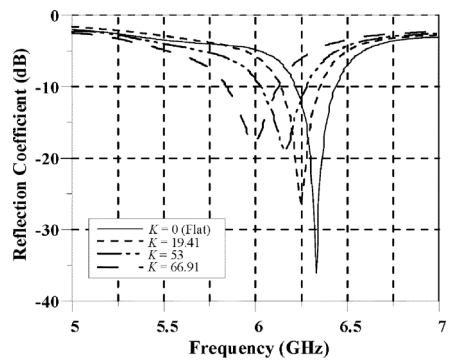

Fig. 8. Measured reflection coefficient of the proposed antenna.

TABLE I
Parameters for Microstrip Patch Antenna

	R (Ω)	L (nH)	C (pF)
$K = 0$	223.6	0.126	5.5
$K = 19.41$	234.73	0.112	6.32
$K = 53$	258.9	0.110	6.55

K increases, which is consistent with the simulation results as shown in Fig. 3. A simple parallel resonant RLC circuit is often utilized to model the microstrip patch antenna. A few works have been done to calculate the values of RLC parameters [17], [18]. The extraction of the element parameters of the circuit model from the measured reflection coefficient was conducted using the advanced design system (ADS). The extracted element parameters of the circuit model are listed in Table I. From Table I, it can be observed that as the curvature increases, the capacitance also increases, while the inductance only shows a comparatively minor change. This phenomenon explains the shift of resonant frequency to a lower frequency when K increases.

Radiation pattern measurement is conducted in an anechoic chamber using the HP 85301 vector network analyzer. A polylon mold is made to facilitate the measurement. Figs. 10 and 11 show the simulated and measured radiation pattern of the proposed antenna, respectively. The small ripples shown on the measured radiation pattern are caused by the vibration of the proposed antenna while conducting the measurement. The measured maximum gain of the proposed antenna is 2.17 dBi. The discrepancy between the simulated and measured results should be caused by manufacturing imperfections and measurement errors.

For the flat microstrip patch antenna, the radiation is originated from the fringing E-fields on the edge of the patch that would add up in phase along the direction of x-axis [Fig. 12(a)].

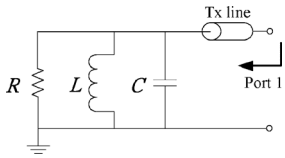

Fig. 9. Equivalent circuit model of the microstrip patch antenna.

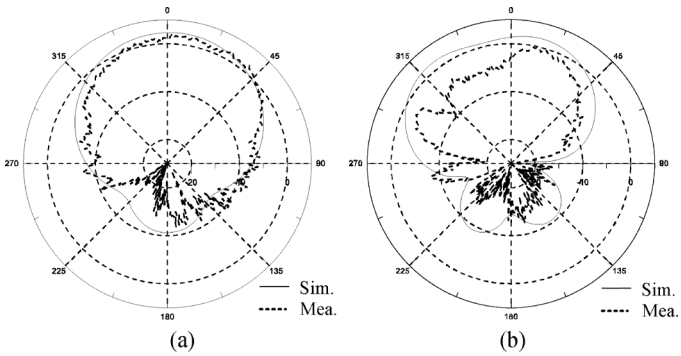

Fig. 10. Simulated (solid curve) and measured (dotted curve) radiation pattern (copolarization components) of the proposed antenna when $K = 19.41$ at 6.25 GHz. (a) yz-plane. (b) xz-plane.

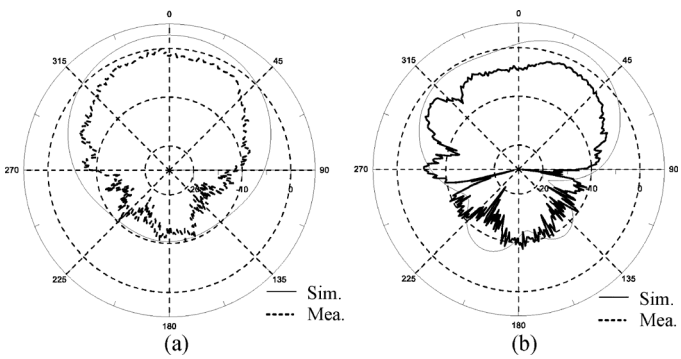

Fig. 11. Simulated (solid curve) and measured (dotted curve) radiation pattern (copolarization components) of the flexible SU-8/PDMS antenna when $K = 53$ at 6.15 GHz. (a) yz-plane. (b) xz-plane.

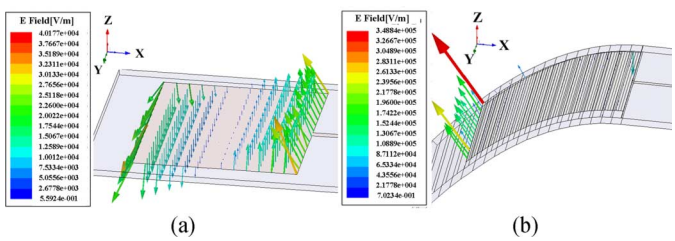

Fig. 12. Simulated E-fields as K equals (a) 0 and (b) 53.

However, in the bent situation [Fig. 12(b)], the fringing E-fields are no longer added up in the same phase in the direction of x-axis. Only the fringing E-fields at the open end of the patch will be responsible for the radiation due to the bending effect. As a result, this phenomenon causes the variation on the radiation pattern in xz-plane.

V. Conclusion

For the first time, we present the design and development of the flexible SU-8/PMDS microstrip patch antenna. The characteristics of the bent antenna have been measured and characterized. Experimental results have shown the bending effects including the frequency shift and the variation on the radiation pattern in xz-plane owing to the reduction of capacitance and the uneven fringing E-fields on the edge of the patch, respectively. The fabrication process of the proposed antenna shows the capability of being able to integrate itself with CMOS chips for flexible RFIC's applications. The next objective is to integrate the proposed flexible antenna with the technology reported previously [10], [11] and develop a fully integrated wireless microsystem.

Acknowledgment

The authors would like to thank the National Center for High-Performance Computing (NCHC) for the support of EM simulator.

References

[1] Y. Sun and J. A. Rogers, "Inorganic semiconductors for flexible electronics," *Adv. Mater.*, vol. 19, pp. 1897–1916, 2007.
[2] Y. Sun and J. A. Rogers, "Inorganic semiconductors for flexible electronics," *Adv. Mater.*, vol. 19, pp. 1897–1916, 2007.
[3] S. Cheng and Z. Wu, "Microfluidic stretchable RF electronics," *Lab Chip*, vol. 10, no. 23, pp. 3227–3234, Sep. 2010.
[4] S. Nikolaou, G. E. Ponchak, J. Papapolymerou, and M. M. Tentzeris, "Conformal double exponentially tapered slot antenna (DETSA) on LCP for UWB applications," *IEEE Trans. Antennas Propag.*, vol. 54, no. 6, pp. 1663–1668, Jun. 2006.
[5] G. DeJean, R. Bairavasubramanian, D. Thompson, G. E. Ponchak, M. M. Tentzeris, and J. Papapolymerou, "Liquid crystal polymer (LCP): A new organic material for the development of multilayer dual-frequency/dual-polarization flexible antenna arrays," *IEEE Antennas Wireless Propag. Lett.*, vol. 4, pp. 22–26, 2005.
[6] N. Tiercelin, P. Coquet, R. Sauleau, V. Senez, and H. Fujita, "Polydimethylsiloxane membranes for millimeter-wave planar ultra flexible antennas," *J. Micromech. Microeng.*, vol. 16, no. 11, pp. 2389–2395, Nov. 2006.
[7] J. So, J. Thelen, A. Qusba, G. J. Hayes, G. Lazzi, and M. D. Dickey, "Reversibly deformable and mechanically tunable fluidic antennas," *Adv. Func. Mater.*, vol. 19, no. 22, pp. 3632–3637, Nov. 2009.
[8] A. Ghannam, C. Viallon, D. Bourrier, and T. Parra, "Dielectric microwave characterization of the SU-8 thick resin used in an above IC process," in *Proc. EuMC*, 2009, pp. 1041–1044.
[9] F. D. Mbairi and H. Hesselbom, "High frequency design and characterization of SU-8 based conductor backed coplanar waveguide transmission lines," in *Proc. ISAPM*, 2005, pp. 243–248.
[10] T.-Y. Chao, C.-W. Liang, Y. T. Cheng, and C.-N. Kuo, "Heterogeneous chip integration process for flexible wireless microsystem application," *IEEE Trans. Electron Devices*, vol. 58, no. 3, pp. 906–909, Mar. 2011.
[11] T.-Y. Chao and Y. T. Cheng, "Wafer-level chip scale flexible wireless microsystem fabrication," in *Proc. IEEE MEMS Conf.*, Cancun, Mexico, Jan. 2011, pp. 344–347.
[12] I. Locher and M. Klemm, "Design and characterization of purely textile patch antennas," *IEEE Trans. Adv. Packag.*, vol. 29, no. 4, pp. 777–788, Nov. 2006.
[13] S. Cheng, A. Rydberg, K. Hjort, and Z. Wu, "Liquid metal stretchable unbalanced loop antenna," *Appl. Phys. Lett.*, vol. 94, no. 14, pp. 144103–144103-3, 2009.
[14] S. Cheng, Z. Wu, P. Hallbjorner, K. Hjort, and A. Rydberg, "Foldable and stretchable liquid metal planar inverted cone antenna," *IEEE Trans. Antennas Propag.*, vol. 57, no. 12, pp. 3765–3771, Dec. 2009.
[15] E. Apaydin, Y. Zhou, S. Koulouridis, J. L. Volakis, and D. Hansford, "Multilayer printing on PDMS-ceramic composites for RF integration and packaging," in *Proc. IEEE APSURSI*, Jun. 2009, vol. 1–5, pp. 1–4.
[16] W. L. Stutzman and G. A. Thiele, *Antenna Theory and Design*. New York: Wiley, 1998.
[17] F. Abboud, J. P. Damiano, and A. Papiernik, "Simple model for the input impedance of coax-fed rectangular microstrip patch antenna for CAD," *Proc. Inst. Elect. Eng. Microw., Antennas Propag.*, vol. 135, no. 5, pp. 323–326, Oct. 1988.
[18] N. M. Martin, "Improved cavity model parameters for calculation of resonant frequency of rectangular microstrip antennas," *Electron. Lett.*, vol. 24, no. 11, pp. 680–681, May 1988.